

## Experiment Report Form

The double page inside this form is to be filled in by all users or groups of users who have had access to beam time for measurements at the ESRF.

Once completed, the report should be submitted electronically to the User Office via the User Portal:  
<https://www.esrf.fr/misapps/SMISWebClient/protected/welcome.do>

### Deadlines for submission of Experimental Reports

Experimental reports must be submitted within the period of 3 months after the end of the experiment.

#### Experiment Report supporting a new proposal (“relevant report”)

If you are submitting a proposal for a new project, or to continue a project for which you have previously been allocated beam time, you must submit a report on each of your previous measurement(s):

- even on those carried out close to the proposal submission deadline (it can be a “*preliminary report*”),
- even for experiments whose scientific area is different from the scientific area of the new proposal,
- carried out on CRG beamlines.

You must then register the report(s) as “relevant report(s)” in the new application form for beam time.

### Deadlines for submitting a report supporting a new proposal

- 1<sup>st</sup> March Proposal Round - **5<sup>th</sup> March**
- 10<sup>th</sup> September Proposal Round - **13<sup>th</sup> September**

The Review Committees reserve the right to reject new proposals from groups who have not reported on the use of beam time allocated previously.

#### Reports on experiments relating to long term projects

Proposers awarded beam time for a long term project are required to submit an interim report at the end of each year, irrespective of the number of shifts of beam time they have used.

#### Published papers

All users must give proper credit to ESRF staff members and proper mention to ESRF facilities which were essential for the results described in any ensuing publication. Further, they are obliged to send to the Joint ESRF/ ILL library the complete reference and the abstract of all papers appearing in print, and resulting from the use of the ESRF.

Should you wish to make more general comments on the experiment, please note them on the User Evaluation Form, and send both the Report and the Evaluation Form to the User Office.

### Instructions for preparing your Report

- fill in a separate form for each project or series of measurements.
- type your report in English.
- include the experiment number to which the report refers.
- make sure that the text, tables and figures fit into the space available.
- if your work is published or is in press, you may prefer to paste in the abstract, and add full reference details. If the abstract is in a language other than English, please include an English translation.



**Experiment title:** Towards Rational Understanding of the Fe-quarterpyridine-mediated CO<sub>2</sub> Reduction

**Experiment number:**  
CH6520

<b>Beamline:</b> ID26	<b>Date of experiment:</b> from: 6/09/2022 to: 12/09/2022	<b>Date of report:</b> 12/09/2022
<b>Shifts:</b> 18	<b>Local contact(s):</b> Blanka Detlefs	<i>Received at ESRF:</i>

**Names and affiliations of applicants** (\* indicates experimentalists):

Dr. Olaf Rüdiger – Group Leader at Max Planck Institute for Chemical Energy Conversion

Dr. Marcos Gil Sepulcre – MSCA fellow at Max Planck Institute for Chemical Energy Conversion

Dr. Christopher Joseph – AvH fellow at Max Planck Institute for Chemical Energy Conversion

## Report:

Initially the plan was to measure the intermediates of the complex  $[\text{Fe}^{\text{II}}(\text{qpy})(\text{H}_2\text{O})_2]^{2+}$ , containing the ligand 2,2':6',2'':6'',2'''-quaterpyridine (qpy). However, we finally decided to focus our attention in a novel promising family of qpy-based Co-catalyst prepared in our laboratory (Chart 1). Among the new family of catalyst, the system functionalized with electron-donating groups,  $[\text{Co}^{\text{II}}(\text{L1})(\text{H}_2\text{O})_2]^{2+}$  is highly active towards CO<sub>2</sub>RR achieving currents of 0.7 mA, which triplicates that of the previously reported  $[\text{Co}^{\text{II}}(\text{qpy})(\text{H}_2\text{O})_2]^{2+}$ . With the objective of fully understanding the mechanism of Co(qpy)-mediated CO<sub>2</sub> reduction to CO we decided of measure the best catalyst of this series,  $[\text{Co}^{\text{II}}(\text{L1})(\text{H}_2\text{O})_2]^{2+}$ , and use the X-ray emission spectroscopy (XES) techniques, K $\beta$  XES, high energy resolution fluorescence detected (HERFD), and Valence-to-Core (VtC) XES to understand the electronic structure, geometry and coordination number of the steady-state intermediates of CO<sub>2</sub>RR. With this goal in mind, we prepared samples of the steady state intermediates of  $[\text{Co}^{\text{II}}(\text{L1})(\text{H}_2\text{O})_2]^{2+}$  at different oxidation states and scaled up the synthesis of the complex to perform operando measurements in solution.

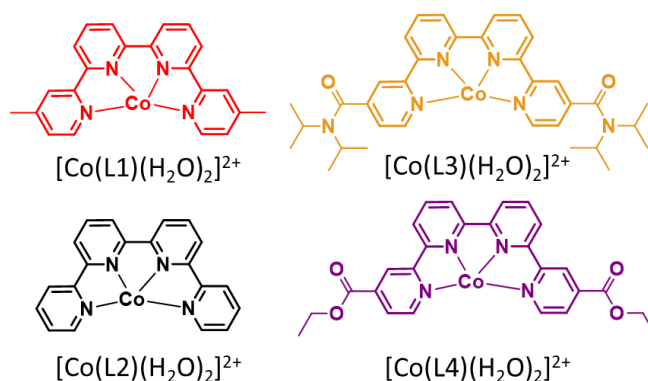


**Chart 1.** Schematic drawing of the complexes discussed in this report.

Firstly, we analyzed the samples containing the  $[\text{Co}^{\text{II}}(\text{L1})(\text{H}_2\text{O})_2]^{2+}$  as a solid and in a solution of propylene carbonate containing 0.1 M of TBAPF6 as supporting electrolyte and 3M of PhOH as proton source to clearly to define the starting point of the catalytic cycle. Interestingly, the measurements show a clear difference between both samples, which are in strong agreement with our electrochemical and X-ray diffraction studies. In case of the sample prepared in solution, a very weak pre-edge (1s-3d) feature suggest that the catalyst displays an octahedral geometry (Figure 1A). This is consistent with the crystals obtained by slow diffusion of Et<sub>2</sub>O under the same conditions (see Figure 1B), which suggest that the species obtained in the crystallization media are the same than the dynamic complex in solution. However, the XANES spectrum of the powder shows completely different features, which can be explained by the fast ligand exchange observed in  $[\text{Co}^{\text{II}}(\text{L1})(\text{H}_2\text{O})_2]^{2+}$  that exchange the axial ligands with the solvent or traces of water in the media. In case of the complex in solution, it coordinates water molecules which are traces in the PhOH. However, when waters are no available it is prone to display a pseudo-octahedral geometry with a  $\text{ClO}_4^-$  as a elongated bond/contact (ca. 2.24 Å) in the axial position (See X-ray structures in Figure 1C). DFT calculations will be carried out to simulate the spectra and fully characterize the electronic structure and geometry of  $[\text{Co}^{\text{II}}(\text{L2})(\text{H}_2\text{O})_2]^{2+}$  in solid state to understand its coordination sphere and geometry.

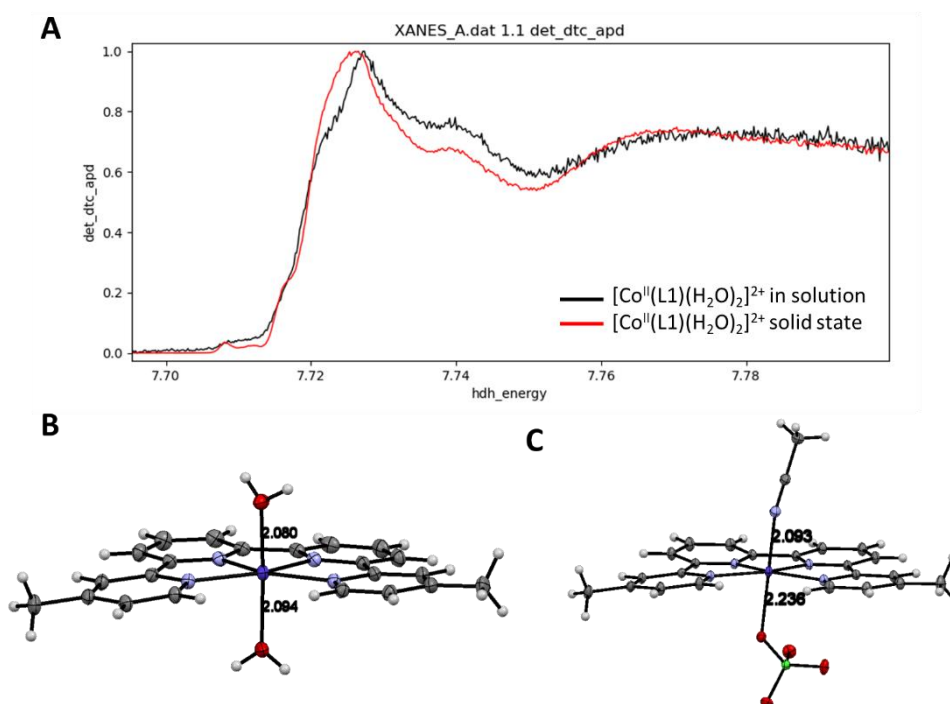
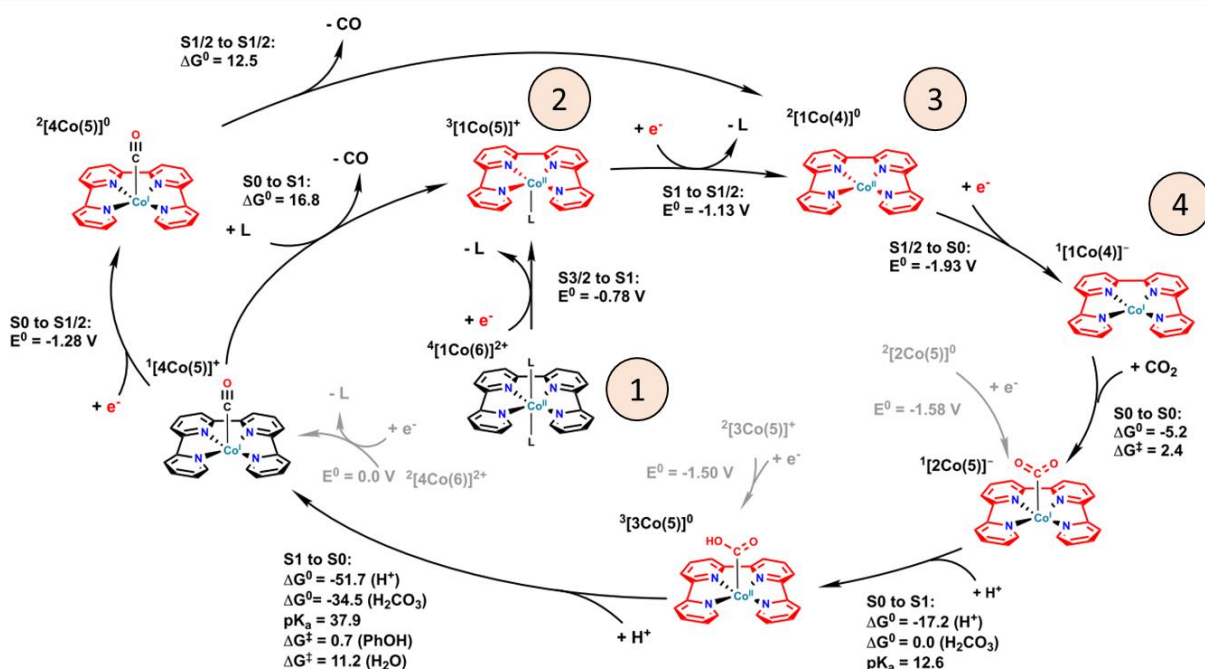


**Figure 1.** (a) HERFD spectra of  $[\text{Co}^{\text{II}}(\text{L1})(\text{H}_2\text{O})_2]^{2+}$  in solid state and in solution recorded with the X-ray emission energy set to 7656eV. (b) X-ray structure of  $[\text{Co}^{\text{II}}(\text{L1})(\text{H}_2\text{O})_2]^{2+}$  crystallized by slow diffusion of Et<sub>2</sub>O in MeCN in absence of water. (c) X-ray structure of  $[\text{Co}^{\text{II}}(\text{L1})(\text{H}_2\text{O})_2]^{2+}$  crystallized by slow diffusion of Et<sub>2</sub>O in a solution of containing 3M of PhOH.

Once the starting point of the catalytic cycle was clarified, we moved to the investigation of reactive intermediates. For this purpose, samples of 1 electron, 2 electron and 3 electron reduced species were prepared by applying the corresponding constant potential to a solution of  $[\text{Co}^{\text{II}}(\text{L1})(\text{H}_2\text{O})_2]^{2+}$  in propylene carbonate containing 0.1 M of TBAPF6 as supporting electrolyte and 3M of PhOH as proton source under Ar atmosphere and in a two-compartment cell. In case of the 1 electron reduced species (2 in scheme 1) a solution was prepared with a concentration of 2 mM. However, a concentration of 0.5 mM was used for 2 electron and 3 electron reduced species (3 and 4 in scheme 1, respectively) due to the fast precipitation of the highly reduced intermediates at mentioned concentrations. K $\beta$  XES, HERFD and Valence-to-Core XES were carried out for all the samples and the results are displayed in Figure 2.

As can be observed in the Figure 2, the reduction of the initial complex (1) to the 1 electron reduce species (2) has a strong effect in the XANES and K $\beta$  XES spectra. The most significant feature is the rise of a 1s to 3d pre-edge feature at ca. 7.71 KeV that suggest a change in the geometry around the metal center. Furthermore, another rising edge feature appears before the white line, both suggest that an axial ligand can decoordinate the metal center changing from octahedral to a square pyramidal geometry. This is in strong agreement with the DFT

studies reported in the literature for the parent  $[\text{Co}^{\text{II}}(\text{qpy})(\text{H}_2\text{O})_2]^{2+}$ .<sup>1</sup> These studies, predicted the formation of an square planar intermediate after one electron reduction to the ligand, which is accompanied with a change in the electronic structure from high to low spin, which is strongly antiferromagnetically coupled. This change is also consistent with the  $\text{K}\beta$  XES spectrum, where a loss of the  $\text{K}\beta''$  feature is observed, probably due to the strongly antiferromagnetically coupled unpaired electrons located at the ligand and metal center. Afterwards, the two electron reduced species was analyzed (3 in Figure 2). The XANES spectrum clearly shows the disappearance of the pre-edge feature, which suggest structural changes around the metal center to a more symmetric conformation. This is consistent with our DFT calculations that shows a favored change from square pyramidal to square planar geometry. Additionally, the edge feature looks shifted to lower energies that could indicate a change in the oxidation state of the metal center from  $\text{Co}^{\text{II}}$  to  $\text{Co}^{\text{I}}$ . Finally, the 3 electron reduced species intermediate (4) was investigated. This intermediate is the responsible to trigger the catalysis and therefore the one that governs the catalytic performance of  $[\text{Co}^{\text{II}}(\text{L1})(\text{H}_2\text{O})_2]^{2+}$ . It is worth mentioning that the isolation of 4 is only possible under Ar conditions and in the total absence of  $\text{PhOH}$ , which in the absence of  $\text{CO}_2$  favors the catalytic hydrogen evolution reaction. The XANES spectra does not show a shift in the edge, which suggest that the oxidation state of the metal center could remain unaltered, and therefore it could suggest that a second reduction in the ligand triggers the catalysis. In order to get more information, the spectra obtained for 4 will be compared with other experiments, such as EPR, UV-vis and NMR (expected  $S=0$ ) and other techniques to propose the structure of the key intermediate.



**Scheme 1.** Mechanism for the selective  $\text{CO}_2$  to  $\text{CO}$  reduction using  $[\text{Co}^{\text{II}}(\text{qpy})(\text{H}_2\text{O})_2]^{2+}$  proposed by M. Head-Gordon et. al. Orange and red colored structures indicate the presence of radicals or excess of electrons on the qpy ligand and others, respectively. Gray arrows indicates proposed competitive pathways. S indicates calculated electronic spin state of each intermediate, respectively.

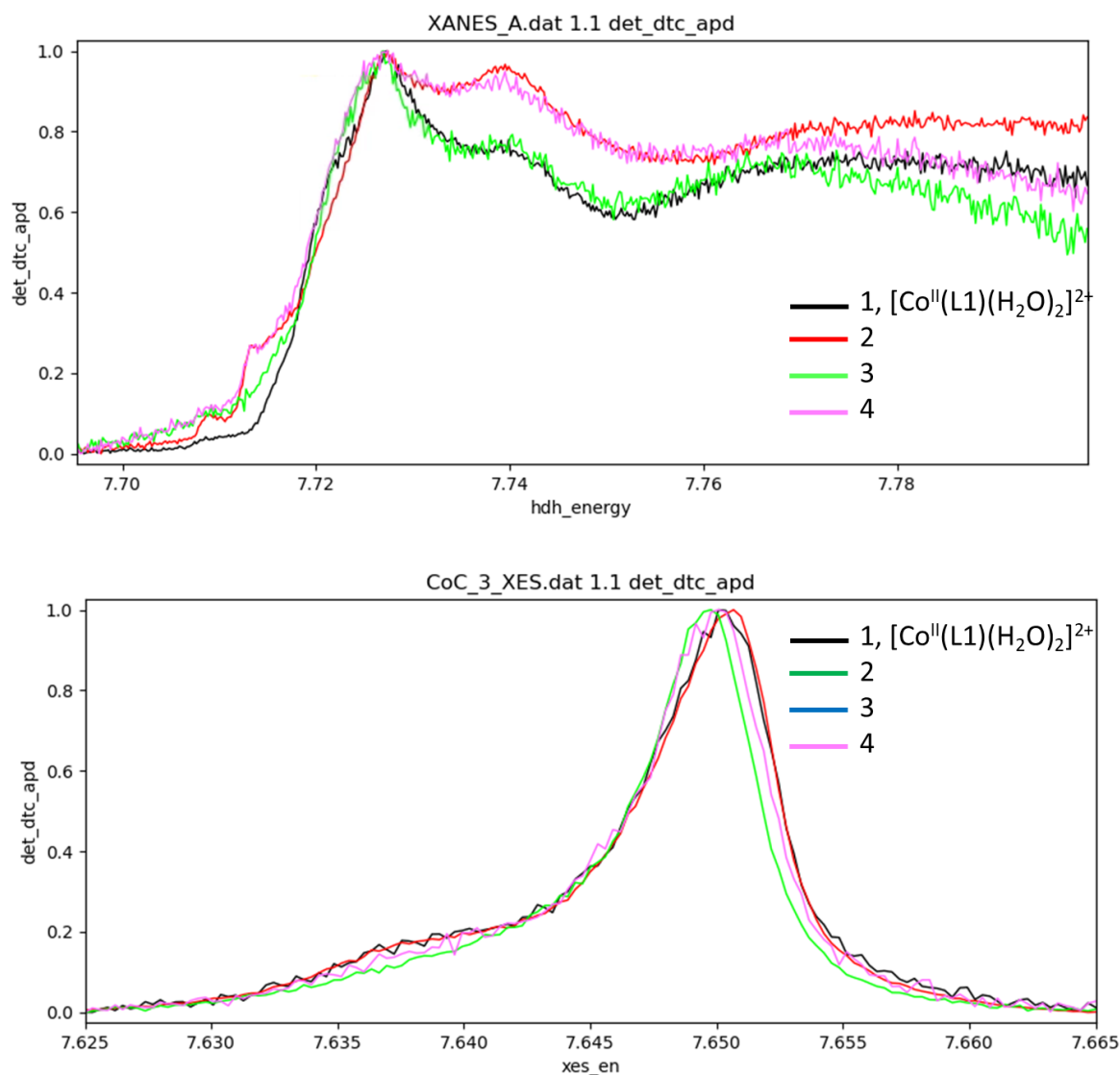


**Figure 2.** HERFD spectra of reaction intermediates 1-4 for  $[\text{Co}^{\text{II}}(\text{L1})(\text{H}_2\text{O})_2]^{2+}$ . K $\beta$  main lines XES of reaction intermediates 1-4 for  $[\text{Co}^{\text{II}}(\text{L1})(\text{H}_2\text{O})_2]^{2+}$ .

Additionally, VtC XES spectra of 1-4 were recorded to further probe the electronic structure of the intermediates. The results are displayed in the Figure 3, and we should compare them with DFT calculations before getting conclusions. VtC XES experiments will help to follow changes in the first coordination sphere and differentiate between  $\text{CO}_2$  or  $\text{CO}$  coordinating the metal center in the intermediates 1-4.

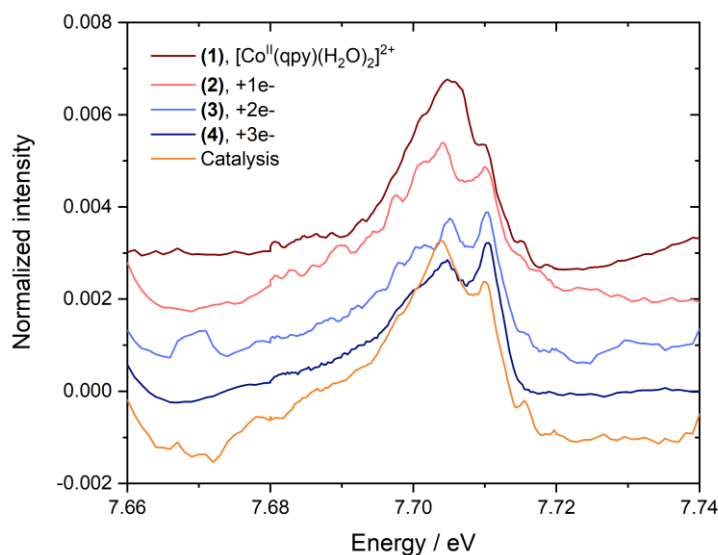


**Figure 3.** VtC XES of reaction intermediates 1-4 for  $[\text{Co}^{\text{II}}(\text{L1})(\text{H}_2\text{O})_2]^{2+}$  and under catalysis.

Additionally, the electronic structure of the proposed resting state of the catalysis was investigated by preparing a sample during the catalytic experiment at  $t = 2\text{h}$ . Comparison of the XANES spectrum with **1**, displayed in the Figure 4, shows that the species that remains as resting state of the catalysis is the one-electron reduced species, which is in strong agreement with our catalytic proposal displayed in Scheme 1. Moreover, the stability of the system was checked. For this purpose, the species in solution were reduced again to the initial compound  $[\text{Co}^{\text{II}}(\text{L1})(\text{H}_2\text{O})_2]^{2+}$  (**1**) and the XANES and  $\text{K}\beta$  XES spectra were compared. The comparison shows the same spectra for  $[\text{Co}^{\text{II}}(\text{L1})(\text{H}_2\text{O})_2]^{2+}$  before and after the catalytic process, which demonstrates the robustness of our catalyst and dismisses the degradation to metallic cobalt-based nanomaterials.

Finally, we attempted to carry out *operando* measurements in solution. For this purpose, a custom-made spectroelectrochemical (SEC) flow-cell was used. The SEC cell uses a glassy carbon plate (2 x 1 cm and 180  $\mu\text{m}$  thick) as working electrode. A solution of  $[\text{Co}^{\text{II}}(\text{L1})(\text{H}_2\text{O})_2]^{2+}$  was bubbled with  $\text{CO}_2$  and pumped through the cell filling the compartment. A potentiostat was used to keep a constant potential from -0.95 to -0.90 V at the catalytic wave and a constant flow of 40-100  $\mu\text{L}/\text{min}$  was used. Unfortunately, we found that *operando* measurements in homogeneous conditions were not possible due to the fluctuations on the concentration provoked by the formation of  $\text{CO}$  bubbles. This strongly affects the accumulation of scans in the detector, which is translated in spikes and variations between recorded spectra. After measuring 100 scans for the XANES spectrum, only 15 were usable. However, we could not collect the  $\text{K}\beta$  and VtC XES due to this reason. To overcome this challenge, we propose two alternative experiments for the future. On the one hand, we can use a cryostream to freeze the homogeneous spectro-electrochemical cell during catalysis, and measure the frozen solution. Alternatively, a prepared analog of  $[\text{Co}^{\text{II}}(\text{L1})(\text{H}_2\text{O})_2]^{2+}$  containing pyrene groups,  $[\text{Co}^{\text{II}}(\text{QPYPyn})(\text{Cl})_2]$ , can be anchored to carbon nanotubes (CNTs) through  $\pi$ - $\pi$  interactions and measured under *operando* conditions.

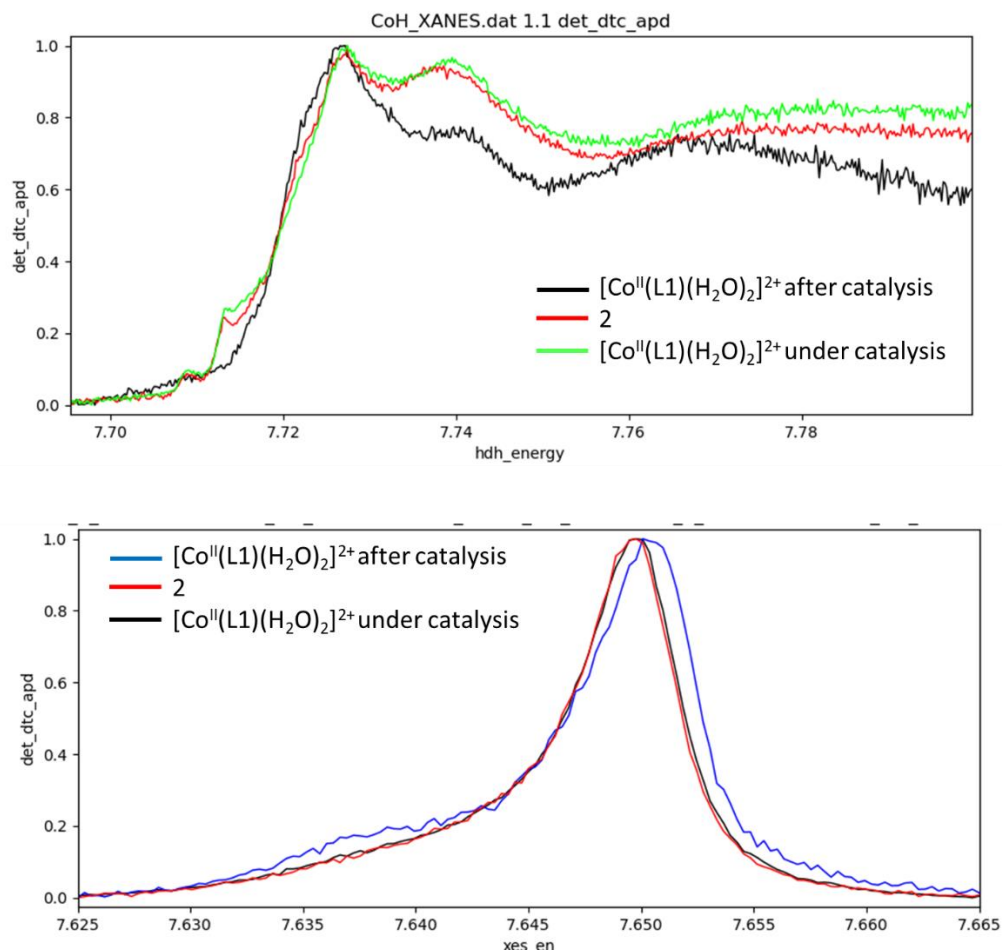


**Figure 4.** HERFD spectra of reaction intermediate 2 and  $[\text{Co}^{\text{II}}(\text{L1})(\text{H}_2\text{O})_2]^{2+}$  during and after catalysis.  $\text{K}\beta$  main lines XES of reaction intermediates 2 and  $[\text{Co}^{\text{II}}(\text{L1})(\text{H}_2\text{O})_2]^{2+}$  during and after catalysis.

In order to take advantage of the time, we installed the cryostat again and we measured  $[\text{Co}^{\text{II}}(\text{L1})(\text{H}_2\text{O})_2]^{2+}$  in acetonitrile as solvent to compare and prove that the experiments performed in propylene carbonate and the same that the ones performed in MeCN (where the catalysis takes place).

All these conclusions are preliminary and they should be compared with EPR, UV-vis and electrochemical measurements performed at MPI. Moreover, all the structures and intermediates reported here will be optimized and their spectra will be simulated by DFT calculations.

<sup>i</sup> M. Loipersberger *et al.* *J. Am. Chem. Soc.* **2021**, *143*, 744.